

DEPARTMENT OF MECHANICAL ENGINEERING & MECHANICS  
COLLEGE OF ENGINEERING & TECHNOLOGY  
OLD DOMINION UNIVERSITY  
NORFOLK, VIRGINIA 23529

LANGLEY  
GRANT  
IN-24-CR

**TOUGHENING OF PMR COMPOSITES BY  
SEMI-INTERPENETRATING NETWORKS**

53062  
P30

By

K. Srinivansan, Research Associate

and

S. N. Tiwari, Principal Investigator

Final Report

For the period ended September 30, 1991

Prepared for

National Aeronautics and Space Administration

Langley Research Center

Hampton, Virginia 23665

Under

**Research Grant NAG-1-569**

Robert M. Baucom, Technical Monitor

MD-Polymeric Materials Branch

(NASA-CR-189468) TOUGHENING OF PMR  
COMPOSITES BY SEMI-INTERPENETRATING NETWORKS  
Final Report, period ended 30 Sep. 1991  
(Old Dominion Univ.) 30 p CSCL 110

N92-15129

Unclas  
G3/24 0053062

November 1991

DEPARTMENT OF MECHANICAL ENGINEERING & MECHANICS  
COLLEGE OF ENGINEERING & TECHNOLOGY  
OLD DOMINION UNIVERSITY  
NORFOLK, VIRGINIA 23529

**TOUGHENING OF PMR COMPOSITES BY  
SEMI-INTERPENETRATING NETWORKS**

By

K. Srinivansan, Research Associate

and

S. N. Tiwari, Principal Investigator

Final Report

For the period ended September 30, 1991

Prepared for

National Aeronautics and Space Administration

Langley Research Center

Hampton, Virginia 23665

Under

**Research Grant NAG-1-569**

Robert M. Baucom, Technical Monitor

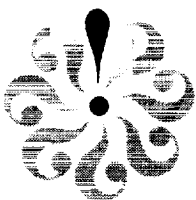
MD-Polymeric Materials Branch

Submitted by the

**Old Dominion University Research Foundation**

**P.O. Box 6369**

**Norfolk, Virginia 23508-0369**



November 1991

1

## FOREWORD

This is a final report on the research project, "Chemoviscosity Modeling for Thermosetting Resins," for the period ended September 30, 1991. Special attention during this period was directed to the study of "Toughening of PMR Composites by Semi-Interpenetrating Networks." The work was supported by the NASA Langley Research Center (Polymeric Materials Branch of the Materials Division) under the grant NAG-1-569. The grant was monitored by Mr. Robert M. Baucom.

# TOUGHENING OF PMR COMPOSITES BY SEMI - INTERPENETRATING NETWORKS

K. SRINIVASAN\* AND S. N. TIWARI\*\*

## ABSTRACT

Polymer composites are increasingly being required to operate for prolonged durations at high temperatures. In the past, the material of choice for most elevated temperature applications was PMR - 15, even though it suffered from two major drawbacks : brittleness and component toxicity. Recently, there have been increased efforts devoted to synthesizing and characterizing new, non - toxic polymers capable of withstanding high temperatures for long periods. Several such organic polymers have been investigated. One such potential PMR - 15 replacement is LaRC RP46. Further, to improve the damage tolerance of PMR - type resin systems, an attempt has been made to develop a semi - Interpenetrating Network (semi - IPN) at ply interfaces by utilizing a tough thermoplastic resin. Matrimid 5218 (Ciba Geigy) is a tough thermoplastic polyimide with a  $T_g$  of  $315^\circ\text{C}$  -  $325^\circ\text{C}$ , a range compatible with PMR - type composites. A controlled creation of a 5218 / PMR semi - IPN at the ply - to - ply interface is therefore likely to provide toughness to the resulting composite without substantial loss of high temperature capability.

PMR - 15 and RP46 prepregs were drum wound using IM - 7 fibers. Prepregging and processing conditions were optimized to yield good quality laminates with fiber volume fractions of 60 percent ( $\pm 2$  percent). Samples were fabricated and tested to determine comprehensive engineering properties of both systems. These included  $0^\circ$  Flexure, Short Beam Shear, Transverse Flexure and Tension,  $0^\circ$  Tension and Compression, Intralaminar Shear, Short Block Compression, Mode I and II Fracture Toughness and Compression After Impact properties. Semi - 2 - IPN toughened PMR - 15 and RP46 laminates were also fabricated and tested for the same properties.

---

\* Research Associate, Department of Mechanical Engineering and Mechanics, Old Dominion University, Norfolk, VA 23529-0247

\*\* Eminent Professor, Department of Mechanical Engineering and Mechanics, Old Dominion University, Norfolk, VA 23529-0247

## TABLE OF CONTENTS

1.	INTRODUCTION	1
2.	EXPERIMENTAL DETAILS	
	2.1 MATERIALS	3
	2.2 PREPREG MANUFACTURE DETAILS	3
	2.3 LAMINATION	4
	2.4 SAMPLE FABRICATION & TEST PROCEDURES	5
3.	RESULTS AND DISCUSSION	
	3.1 MECHANICAL TEST RESULTS	6
	3.2 MORPHOLOGICAL CONSIDERATIONS	7
4.	CONCLUSIONS	9
5.	REFERENCES	10

## LIST OF FIGURES

1.	CURE CYCLE	11
2.	PARTICLE SIZE DISTRIBUTION	12
3.	POWDER DISPENSER ASSEMBLY	13
4.	POWDER DISPENSER DETAILS	14
5.	PREPREG SEM PHOTOMICROGRAPH	15
6.	STRENGTH DATA	16
7.	STRENGTH DATA	17
8.	MODULUS DATA	18
9.	FAILURE STRAIN / DEFLECTION DATA	19
10.	FRACTURE TOUGHNESS DATA	20

## LIST OF TABLES

1.	PROCESS STANDARDIZATION DETAILS	21
2.	TEST MATRIX	22

**Interim Progress Report on NAG5-1510  
'Reduced Electrical Bandwidth Receivers  
for Direct Detection 4-ary PPM  
Optical Communication Intersatellite Links'  
for the period April 15 - October 15, 1991.**

*Frederic M. Davidson and Xiaoli Sun*

**Summary**

This interim progress report consists of copies of three reports written for NASA's Flight System Development and Demonstration (FSDD) project on optical intersatellite links. The first report, 'Test results of the PlessCor APD preamplifier for use in the 50 Mbps Q=4 PPM receiver,' was prepared for NASA Goddard Space Flight Center. The second, 'Performance of Q-ary PPM receiver under additive white Gaussian noise,' was prepared at the request of NASA Lewis Research Center for testing the electronic systems for the FSDD project. The third, 'Use of a Bessel lowpass filter as an approximate raised cosine filter,' was written for ~~Galaxy Microsystems, Inc.~~ for raised cosine filter implementation in the FSDD QPPM receiver.

November 1991



## STRATOSPHERIC MINOR CONSTITUENTS

## 9.1 INTRODUCTION

The evidence for increasing concentrations of the source gases (CFC's for Cl and F,  $N_2O$  for N, and  $CH_4$  for H, among others) has been summarized in Chapter 8 of this report. Photochemical models predict that increasing source gas concentrations are also expected to lead to changes in the concentrations of both catalytically active radical species (such as  $NO_2$ , ClO, and OH) and inactive reservoir species (such as  $HNO_3$ , HCl, and  $H_2O$ ). For simplicity, we will refer to all these as trace species. This chapter addresses the question of long-term trends in these trace species.

In particular, we consider two questions associated with trace species concentrations. First, are those species whose concentrations are expected to be increasing actually doing so? Second, are there observed changes in any trace species not expected on the basis of the measured increase in source gases?

The consideration of these questions is difficult because of the limited data base of measurements of stratospheric trace species. In situ measurements are made only infrequently, and there are few satelliteborne measurements, most over a short time span insufficient for trend determination. Instead, ground-based measurements of column content must be used for many species, and interpretation is complicated by contributions from the troposphere or mesosphere or both. In this chapter, we examine existing measurements as published or tabulated; they have not been subjected to the rigorous review that has been applied to the ozone data examined in the bulk of this report.

## 9.2 ODD NITROGEN

The odd nitrogen compounds (N, NO,  $NO_2$ ,  $HNO_3$ ,  $N_2O_5$ , ClONO<sub>2</sub>, and HO<sub>2</sub>NO<sub>2</sub>) are important to the chemical balance that determines stratospheric ozone concentrations. They participate in catalytic reactions and can interfere with catalysis by chlorine, hydrogen, and bromine compounds. Because their principal source is nitrous oxide— $N_2O$ —which is known to be increasing at about 0.2 percent per year (see Chapter 8 of this report), a slow increase in the concentration of odd nitrogen compounds should be expected. This increase is sufficiently slow that no currently measurable changes in stratospheric odd nitrogen compounds are expected to result from it. Superimposed on this should be variations caused by interannual variability of the dynamics that transport odd nitrogen from its source in the middle stratosphere to its sinks, either in the mesosphere or troposphere.

Larger changes or long-term cyclical variations, if they are to occur, would likely have to arise from changes in the amount of odd nitrogen generated elsewhere in the atmosphere. In the upper mesosphere and lower thermosphere, processes involving ions and electrons lead to production of NO, which is then transported down to the stratosphere. This problem has been discussed extensively by Solomon and Garcia (1984b), Jackman et al. (1980), and Callis and Natarajan (1986). It has also been suggested (Ko et al., 1986, and references therein) that lightning may be an important source of odd nitrogen production, especially in the tropical upper troposphere. This odd nitrogen might then be transported into the stratosphere. Thus, changes in the rate of troposphere-stratosphere transport in the Tropics might also lead to changes in stratospheric odd nitrogen content. The rest of this section reviews the measurement evidence for changes in the odd nitrogen compounds.

## AEROSOL ABUNDANCES AND DISTRIBUTIONS

## 10.1 INTRODUCTION

~~In this chapter,~~ The properties of aerosols that reside in the upper atmosphere are described, with special emphasis on the influence these aerosols may have on ozone observation systems, mainly through radiative effects, and on ambient ozone concentrations, mainly through chemical effects. It has long been appreciated that stratospheric particles can interfere with the remote sensing of ozone distribution. Here, the mechanism and magnitude of this interference, and potential spatial and temporal trends in the interference, are evaluated. Separate sections deal with the optical properties of upper atmospheric aerosols, long-term trends in stratospheric aerosols, perturbations of the stratospheric aerosol layer by volcanic eruptions, and estimates of the impacts that such particles have on remotely measured ozone concentrations.

Another section is devoted to a discussion of the polar stratospheric clouds (PSC's). These unique clouds, recently discovered by satellite observation, are now thought to be intimately connected with the Antarctic ozone hole (see Chapter 11). Accordingly, interest in PSC's has grown considerably in recent years. This chapter describes what we know about the morphology, physical chemistry, and microphysics of PSC's.

## 10.2 AEROSOLS IN THE MIDDLE AND LOWER ATMOSPHERE

The global measurement of ozone from orbiting satellites using the spectral signature of Earth's albedo is complicated by the presence of fine light-scattering (and absorbing) particles in the upper atmosphere. If the spatial distribution, size distribution, composition, and morphology of these particles are known, their optical properties can be determined and employed in the calculation of ozone abundances from the raw satellite radiance data. Most ozone-sensing systems are not designed to measure independently the aerosol properties that are required. Accordingly, in cases where aerosol interference is identified as a problem, corrections to the ozone observations may be estimated by using either a standard aerosol model, or coincident aerosol data from other sensors, or reanalysis of the onboard data (through a modified inversion scheme) to deduce the aerosol fields. Thus, several alternatives may be available to correct for the effects of aerosols in data retrieval procedures.

Two principal concerns regarding aerosol effects are noted:

1. Research teams working with the satellite radiance data and inversion schemes should be aware of the types and variations of particles in the upper atmosphere and their general optical properties.
2. Past measurements of ozone, both satellite and ground based, which may have been inadvertently contaminated by aerosol scattering effects, might be recalibrated (if this is possible) to allow more accurate ozone trend analyses.

## 10.2.1 Aerosol Species

Table 10.1 summarizes and compares information on the most prominent atmospheric particulates, including water clouds. Specific types of aerosols may not significantly affect a particular system, or may have been taken into account in designing the system. The general optical properties of aerosol particles are discussed in Section 10.2.2.

## 11.1 INTRODUCTION

In 1985, there was a report (Farman et al., 1985) of a large, sudden, and unanticipated decrease in the abundance of springtime Antarctic ozone over the last decade. By 1987, ozone decreases of more than 50 percent in the total column, and 95 percent locally between 15 and 20 km, had been observed. ~~A change of this magnitude was not predicted by any of the photochemical models.~~ The scientific community quickly rose to the challenge of explaining this remarkable discovery; theoreticians soon developed a series of chemical and dynamical hypotheses to explain the ozone loss. ~~Unfortunately, there were inadequate observational data to differentiate among the different theories. Consequently, field measurement campaigns were quickly organized to determine the chemical composition and physical structure of the springtime stratosphere over Antarctica and test the theories.~~ Three basic theories were proposed to explain the springtime ozone hole:

- (1) ✕ The ozone hole is caused by the increasing atmospheric loading of manmade chemicals containing chlorine (chlorofluorocarbons [CFC's]) and bromine (halons). These chemicals efficiently destroy ozone in the lower stratosphere in the Antarctic because of the special geophysical conditions of an isolated air mass (polar vortex) with very cold temperatures that exist there.
- (2) ✕ The circulation of the atmosphere in spring has changed from being predominantly downward over Antarctica to upward. This would mean that ozone-poor air from the troposphere, instead of ozone-rich air from the upper stratosphere, would be transported into the lower Antarctic stratosphere.
- (3) ✕ The abundance of the oxides of nitrogen in the lower Antarctic stratosphere is periodically enhanced by solar activity. Nitrogen oxides are produced in the upper mesosphere and thermosphere and then transported downward into the lower stratosphere in Antarctica, resulting in the chemical destruction of ozone.

~~This chapter discusses the climatology and trends of ozone, temperature, and polar stratospheric clouds; the transport and chemical theories for the Antarctic ozone hole; and the observational evidence to test the different theories.~~

## 11.2 OBSERVATIONS

### 11.2.1 Ozone Climatology and Trends

Until recently, attention has focused primarily on the Antarctic springtime variations in total ozone; however, many questions have arisen concerning the overall seasonal and year-to-year variations throughout the Southern Hemisphere. October is the month originally emphasized by Farman et al. (1985) because it is the month of most dramatic effect. This section will discuss the spatial and temporal extent of the changes in both the total column content and the vertical distribution of ozone over and around Antarctica. Ozone changes from year to year, and within a single year, are addressed. The Total Ozone Mapping Spectrometer (TOMS) data shown in this chapter have not been corrected for the drift against the Dobson network, which has been discussed in great detail in earlier chapters. The drift of TOMS data with respect to the Dobson network was reported to be approximately 0.4 percent per year, which corresponds to a total drift of about 3.6 percent from launch in late 1978 to the present.

## 1.0 INTRODUCTION

In recent times, the need for increased temperature capabilities of polymer composites, has focussed attention on polyimide based systems. Most common among the polyimides for high temperature industrial and structural applications is PMR - 15. With a reported upper use temperature of about 315 ° C, PMR - 15 has several attractive attributes, such as good thermo-oxidative stability, relatively easy processing and low cost and multiple source availability. However, it suffers from two main drawbacks : brittleness and potential toxicity of one of the reactant components.

A lack of toughness, not uncommon among highly crosslinked systems, has severely limited the applications of PMR - 15. Composites made of PMR - 15 exhibit widespread microcracking and very low fracture toughness, particularly during impact and thermal cycling. Several general techniques exist to alleviate this problem. These include toughened resin formulations, through-the-thickness reinforcement and interleaving. The most commonly employed technique for resin toughening is reformulation, particularly by elastomeric and / or thermoplastic modifications. While the impact resistance of such systems is improved, this occurs at the expense of mechanical properties, specifically those relating to hot / wet performance. Interleaving allows for the incorporation of discrete layers of a tough resin between the plies of a composite, thus selectively toughening the highly stressed regions. Such a structure has been shown to be effective in reducing impact damage and increasing post-impact-compressive properties in both epoxy and bismaleimide based composites. Key factors that influence the selection of interleaving agents are toughness, compatibility and use / consolidation temperatures. Through - the - thickness reinforcement involves stitching / weaving / braiding operations, which are currently experimental in nature, difficult to process and lead to a trade - off in other properties.

The health and safety aspects of PMR - 15 focus on one of the bifunctional monomers in the formulation : 4,4' methylenedianiline (MDA). Suspected of being a potential human carcinogen, many researchers feel that controls restricting human exposure to free MDA are imminent. Several alternative approaches to overcome this problem have been proposed, and are detailed in Reference 1. A new potentially low toxic PMR - type system has been recently formulated at NASA Langley Research Center (1). This polyimide designated RP46 was prepared by replacing the MDA with 3,4' oxydianiline (ODA). Some superior properties such as better flow

characteristics, a broader processing window and moderately higher toughness were noted (1).

While both the interleaving / reformulation of epoxy based composites has yielded great success (2 - 4), the toughening of brittle polyimides such as PMR - type composites has not yet been fully exploited. This paper presents the results of a study undertaken to toughen PMR - type composites by selectively toughening ply - to - ply interfaces. In order to make valid comparisons between toughened and non - toughened composites, the laminate fiber volume fraction was kept constant, in both the baseline and toughened composites, by adjusting the resin content of the prepregging solution. This entailed considerable scale-up and process standardization work with the resin systems. In addition to toughness data, a comprehensive engineering property profile evaluation of all systems was undertaken in order to understand the trade - offs involved with the toughening of PMR - type polyimide resins.

## **2.0 EXPERIMENTAL DETAILS**

### **2.1 Materials**

The base resins utilized in this study were PMR -15 and LaRC RP46. The chemistry of both systems has been previously detailed extensively. Both resin systems were synthesized in house. Unsized IM - 7 12K Carbon fiber was selected as the reinforcing fiber. Matrimid 5218 (from Ciba-Geigy) was selected as the toughening agent. It was supplied as fully imidized flakes and was ground to a fine powder using a Retsch Grinder. The particle size distribution is shown in Figure 2. Selection of Matrimid 5218 was based on the following factors. In order to be effective, the toughening agent must have a  $T_g$  close to the processing (crosslinking) temperatures of both PMR - 15 and RP46, so as to not appreciably lower the use temperatures of the composite systems and yet be co-processible with them to fabricate the composite laminate. It must also be stable for prolonged periods at the processing temperatures. A DSC scan of the 5218 powder indicated a  $T_g$  of about 320 ° C. Further, Matrimid 5218 is physically compatible with the base resins at elevated temperatures, and provides good quality, void-free laminates.

### **2.2 Prepreg Manufacture Details**

All materials were impregnated using the drum winding technique. Though this apparatus has been described previously (5), a brief description of the process is outlined. An IM - 7 (12K, unsized) fiber tow from a free spinning unwinding creel, passed between two tension bars and onto guide spools (that aligned the fiber) before it entered a sealed resin reservoir. Within the reservoir, the fiber tow passed through the impregnating solution over an assembly of rollers. These served to spread the fibers as it was being impregnated and ensured complete wetout. The tow exited the reservoir through a stainless steel die that squeezed the resin solution through the fiber tow, metered the amount of resin on the fiber and shaped the thickness and width of the impregnated tow. This tow was wound on a 2.5 feet diameter drum backed with a trifluoroethylene polymer release film. The entire creel - guide roll - reservoir assembly was maintained on a moving track whose translational speed was adjusted such that the impregnated tow wound on the drum to provide a continuous gap-free prepreg. A typical run yielded a 35 square foot sheet of prepreg.

PMR - 15 and RP46 resin solutions of differing concentrations were carefully synthesized and characterized, with respect to various parameters such density and viscosity. These were prepregged and

processed into laminates of different thicknesses and layups. Temperature, pressure and bleed times were optimized to produce laminates with a maximum void content of 1 percent. An insitu high temperature soak cycle was developed to eliminate the long, free standing postcure associated with these systems (Figure 1). Extensive volume fraction measurements of these laminates were undertaken using the chemical digestion method. These results, (for *eg.*, RP46 data summarized in Table 1), were used to determine optimum prepregging and consolidation conditions for producing laminates with fiber volume fractions of approximately 60 percent ( $\pm 2$  percent) and void volumes of less than 1 percent.

In the case of the toughened material, in order to obtain large quantities of controlled, semi - 2 IPN PMR - 15 and RP46 prepreg, several impregnation technologies were evaluated. This resulted in the development of a reproducible, quantitative technique for powder coating prepregs during impregnation, for which a patent disclosure has been filed. In this technique, the 5218 powder was metered onto the wet tow during the impregnation step. This was achieved by mounting a powder filled conical hopper fitted with a central stirrer rod just above the tow as it wound around the drum. An elastomeric nipple was fitted to the hopper at the exit port. The 5218 powder dispensed onto the prepreg was metered by adjusting the annulus between the stirrer rod and the nipple, which could be varied by choosing among several sized nipples. This is shown schematically in Figures 3 and 4. In order to effect a suitable comparison with baseline properties of PMR - 15 and RP46 composites, the resin content of the prepregging solution was adjusted to provide a total resin volume content of 40 percent in both the toughened and non - toughened postcured composites. The 5218 powder metered on the prepreg was approximately 12 percent by weight of the total resin content of the B - staged prepreg. The 5218 powder coalesced / reacted during lamination to give a void free resin layer at the ply interfaces. An SEM photomicrograph of the powder coated RP46 prepreg is shown in Figure 5.

### 2.3 Lamination

The solution wound prepreg remained on the drum for several hours to allow most of the methanol to evaporate. The prepreg was then cut into suitable sizes and B - staged in an air oven at 200 ° C for one hour to remove residual solvent and initiate the chemical reaction to the preimidized polymer. The prepreg was then cut and stacked in the desired layup and thickness, backed with XK 22 release agent coated Kapton films and placed in a matched - metal mold. In order to

eliminate batch - to - batch variations, pieces of prepreg from several batches were incorporated in each laminate. The mold was placed between the platens of a 50 ton four - post upacting press and subject to the cure cycle prescribed in Figure 1. All panels were scanned ultrasonically so as to ensure defect - free laminates for the mechanical testing. The  $T_g$ s of the cured laminates, detected by TMA runs, were as follows :

PMR - 15 : 325 ° C  
Toughened PMR - 15 : 290 ° C  
RP 46 : 325 ° C  
Toughened RP46 : 285 °C.

## 2.4 Sample Fabrication and Test Procedures

The test matrix employed in this study is given in Table 2. Table 2 also provides the laminate layups, sample dimensions and test conditions employed for each of the laminate level property determinations. End - tabbed samples were bonded with 0 / 90 balanced fiberglass laminated end - tabs (G - 10, from Reed Plastics) using Hysol 9309 adhesive. Wherever called for, commercially available room temperature strain gages from Micromeasurements Inc. were employed. All tests were performed in accordance with standardized procedures (ASTM, SACMA).



### 3.0 RESULTS AND DISCUSSION

#### 3.1 Mechanical Test Results

Figures 6 - 10 depict the mechanical properties of all four systems. The error bars represent one standard deviation from the mean. The flexural strengths of the toughened systems were lower than those of the untoughened systems by about 15 - 20 percent. However the flexural strength of the toughened RP46 composite was only marginally lower than that of the PMR - 15 composite, as the RP46 systems showed greater flex strengths than their PMR - 15 counterparts. Flexural modulus like the strength, showed moderate decline with the incorporation of 5218 toughener for both systems. The failure deflection, a measure of toughness in flexure, showed an increase with the addition of toughener. Short Beam Shear strength was also seen to decrease with the incorporation of 5218 toughener.

Unidirectional laminate tensile properties were heavily dominated by fiber properties. Strength, failure strain and modulus data for all systems were consistent with rule - of - mixtures expectations for IM - 7 fiber based composites. However Poissons Ratios appeared to be high for all four systems.

Unidirectional composite compression strength declined modestly (approximately 5 percent) in toughened systems, while failure strain increased. RP46 based composites showed higher compressive strength values than the PMR - 15 based composites. The compressive modulus was unaffected by toughening. Again, Poissons Ratio values appeared to be higher than expected.

In the transverse tension data, scatter was seen to be high, reflective of internal random flaw dominated behavior. No clear correlations emerged from either strength or ultimate strain data. Modulus values were considerably lower than expected values from similar tests on epoxy / PEEK materials.

As a result of the toughening, inplane shear strength values were seen to drop by approximately 15 percent, while modulus values were lower by 10 percent. Compressive properties of quasi - isotropic samples were determined by short block compression tests. Toughening depressed compression strength by 10 - 15 percent, without affecting modulus or ultimate strain values.

Mode I and II fracture toughness values were determined by DCB and ENF specimens respectively. Though the initiation values are

influenced by the thickness of the starter flaw, both Mode I and II initiation fracture toughness values increased with the addition of 5218. Likewise, steady state  $G_c$  values in both Mode I and II increased in the toughened states. RP46 composites showed higher toughness than PMR - 15 composites in initiation and steady state  $G_c$  values in both Mode I and II. Initiation  $G_c$  values were higher than steady state  $G_c$  values in Mode II, but lower in Mode I. While toughening increased steady state Mode I and Mode II  $G_c$  only modestly (20 - 25 percent), the most dramatic improvement was seen in Mode II initiation  $G_c$  values.

### 3.2 Morphological Considerations

Studies were undertaken to determine the morphology of the toughened PMR -15 and RP46 composites. Extensive SEM observations of fractured surfaces in both the toughened composites showed a single phase material. The fracture surfaces were quite tortuous, with grooves, holes and matrix lacerations, but even extensive tilt operations in the SEM did not reveal two separate phases as may be expected from a combination of thermoplastic and thermoset matrices. No evidence of a film or phase was evident at the ply - to - ply interfaces. Fracture surfaces showed evidence of good fiber - resin adhesion.

Thermomechanical runs (TMA) on toughened PMR - 15 and RP46 laminates showed only a single transition in both figures, reflective of a single phase morphology.

Attempts were made to leach out the thermoplastic 5218 resin in both toughened composites. Composite samples were placed in contact with solvents known to dissolve 5218, such as, methylene chloride, chloroform, dioxane, dimethyl formamide, cyclohexanone, dimethyl acetate and N - methyl pyrrolidone, for varying periods of time upto 48 hours. No appreciable weight changes were noted. SEM observations also failed to reveal any leached polymer.

From these observations the morphological picture (of the toughened composites) that emerges is that of a single phase semi - interpenetrating morphology. Given the conditions of laminate fabrication (stacking of PMR - 15 / RP46 prepreg pieces coated with 5218 powder), this leads to several interesting conclusions on the morphology developed in such samples. During the cure cycle, the thermosetting component (PMR - 15 or RP46) continuously increases molecular weight by crosslinking, while the thermoplastic component

(5218) remains relatively chemically inert. This process of cure in the thermosets is accompanied by a viscosity profile that initially decreases with time (due to the rising temperatures) until a trough is reached, after which the viscosity increases (due to increasing molecular weight weight buildup). The 5218 component however, has been processed to a desired molecular weight distribution prior to incorporation in the prepreg, and hence, initially, has a much higher viscosity than the thermosetting component. It is therefore reasonable to presume that the formation of the single phase semi - IPN morphology is initiated by the flow of the PMR - 15 / RP46 component into the 5218 dominated region at each ply - to - ply interface. Since this is a diffusion phenomenon, the interface region is likely to be marked a concentration gradient, with 5218 and thermoset dominated regions at each end and a varying concentration in between. However, since the miscibility of the two components is excellent over the entire range (in this case 0 - 12 percent), no phase segregation occurs, and a single phase semi - IPN morphology is observed.

From a mechanical standpoint, a key requirement for toughness in a composite, is the suppression of delamination, which is a local or global separation of adjacent plies in a laminate. Thus it is critical to selectively toughen the ply - to - ply interface where the stresses are quite high. While a purely tough thermoplastic interleaf may toughen the interface, the resulting composite can be vulnerable to attack by solvents. A semi - IPN at the ply - to - ply interface (with a tough thermoplastic), is likely to provide not only improved toughness and solvent resistance, but also better fatigue endurance and creep resistance, due to enhanced chemical crosslinks that hold the polymer chains together. In this manner, by localizing the toughening agent at the most desired location and by providing crosslinked semi - IPN morphologies, toughening of the bulk resin is avoided, considerably alleviating cost, processing and elevated temperature property problems as well as providing potential for enhanced solvent resistance, creep and fatigue properties.

#### **4.0 CONCLUSIONS**

A manufacturing science outline for the scale up of composites with experimental resin systems has been developed. Careful control of the resin solids content in prepregging solutions, (monitored by solution viscosity), can lead to laminates with controlled volume fractions of resin and fiber. An effective, alternate cure cycle has been devised for PMR - type composites. Based on the results of this methodology, approximately 50 laminates (of different thicknesses and layups) were manufactured with  $V_f = 60$  percent ( $\pm 2$  percent) and a void content of approximately 1 percent, for a comprehensive study of the engineering properties of such systems.

The inherent flexibility of the ether link in 3,4' ODA apparently imparts better flow characteristics and moderately higher toughness to RP46 composites as compared to PMR - 15 composites. This increased toughness is obtained at no sacrifice in engineering strengths and stiffnesses. These factors combined with the lower health risks associated with 3,4' ODA provide an attractive combination of properties for high temperature aerospace and aeroengine applications, including replacement of the PMR - 15 market.

A methodology for selectively toughening ply - to - ply interfaces in PMR - type composites using gradated semi - IPN morphology has been outlined. PMR - 15 and RP46 composites toughened by 5218, show enhanced toughness with small attendant dropoffs in engineering strength and stiffness. Such toughened systems can be processed into thick, multiangle composites with ease.

## **REFERENCES**

1. R. H. Pater, "The 316 ° C and 371 ° C Composite Properties of an Improved PMR Polyimide : LaRC RP46", 36th International SAMPE Symposium, April 15 - 18, 1991, San Diego, CA.
2. J. E. Masters "Improved Impact and Delamination Resistance Through Interleafing", Key Engineering Materials, volume 37, 1989, pp 317 - 348, Trans Tech Publishers, Switzerland.
3. A. F. Yee and R. A. Pearson,
  - a) "Toughening Mechanisms in Elastomer - Modified Epoxy Resins - Part I", NASA CR 3718, August 1983.
  - b) "Toughening Mechanisms in Elastomer - Modified Epoxy Resins - Part II", NASA CR 3852, December 1984.
4. G. R. Almen, P. MacKenzie, V. Malhotra, R. K. Maskell, P. T. McGrail and M. S. Sefton, "Thermoset / Thermoplastic Alloys : An Approach to Tough High Performance Resin Matrices", 20th International SAMPE Technical Conference, September 27 - 29, 1988, Boston, MA.
5. M. L. Wilson and C. E. Stanfield, "Apparatus for Impregnation of Weak Fibers", NASA Technical Briefs, May 1989, pp 84 - 85.

# CURE CYCLE

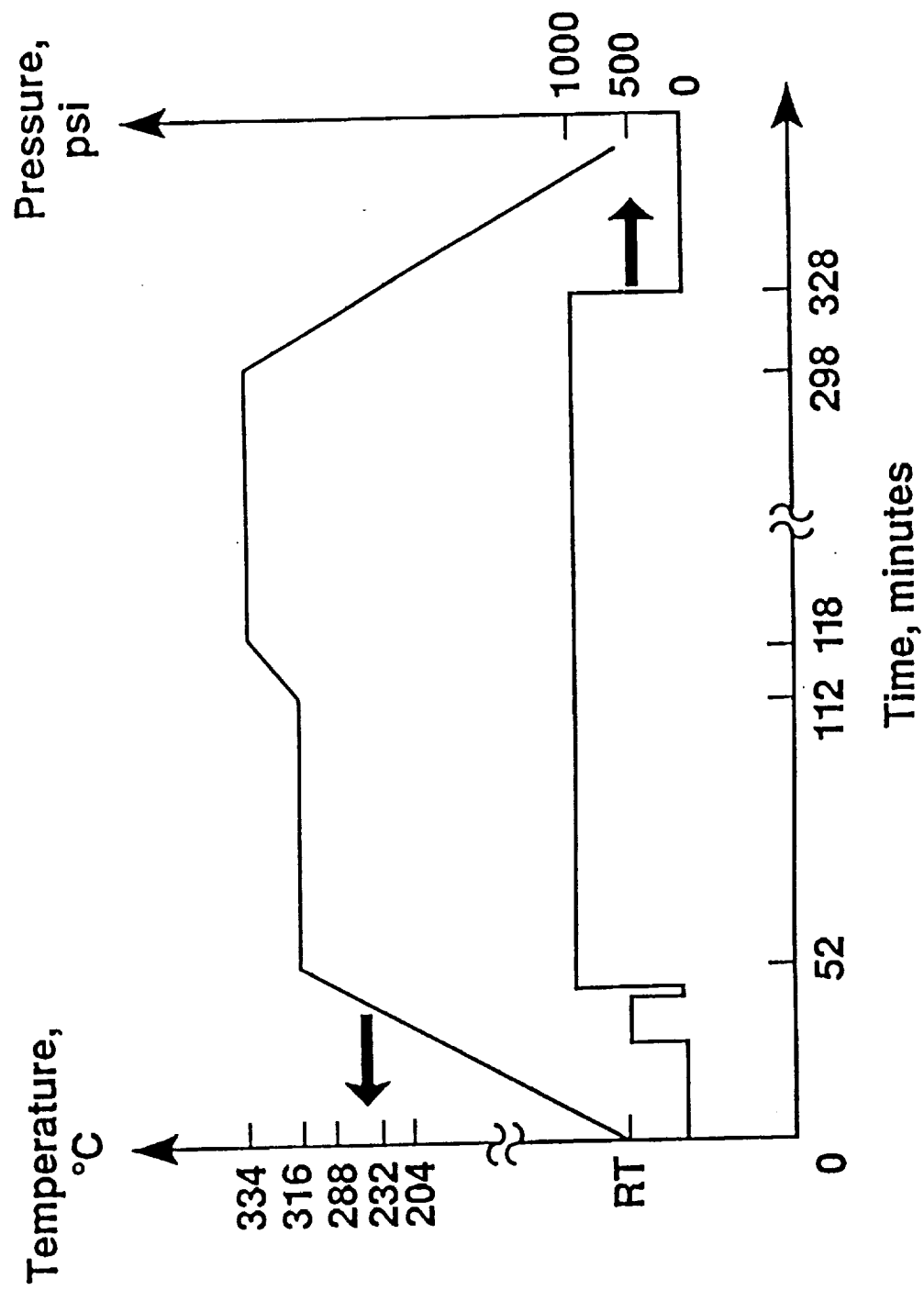


FIGURE 1

# PARTICLE SIZE DISTRIBUTION DATA FOR MATRIMID 5218 POWDER

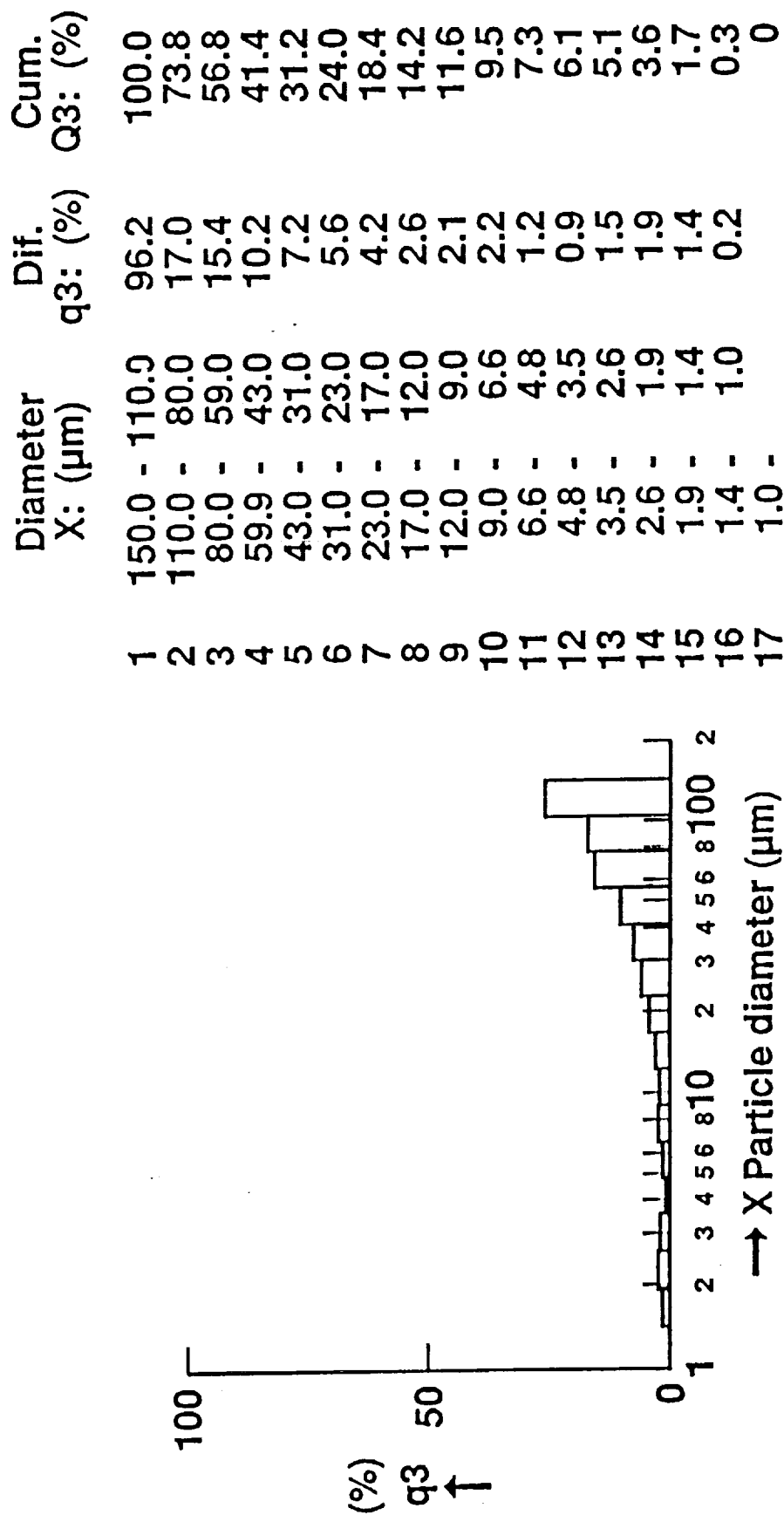
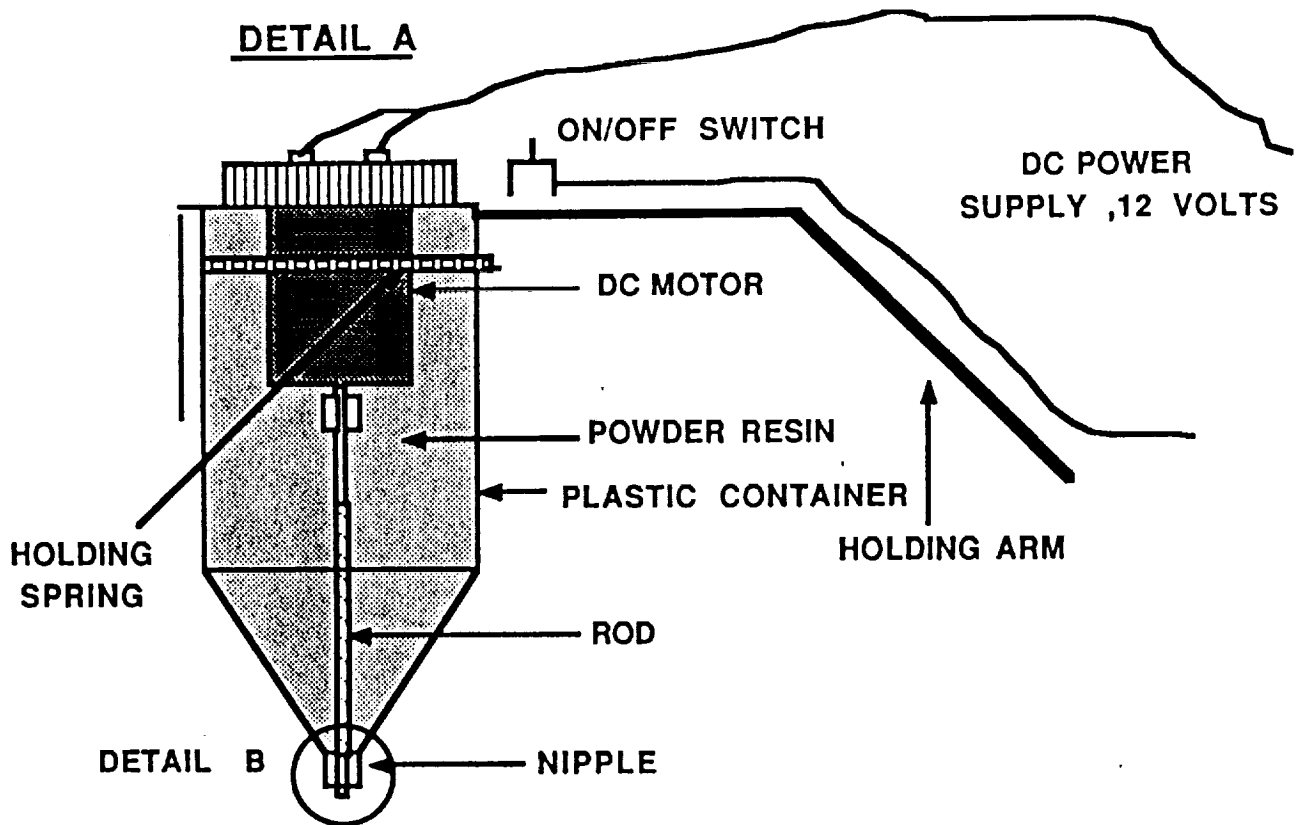
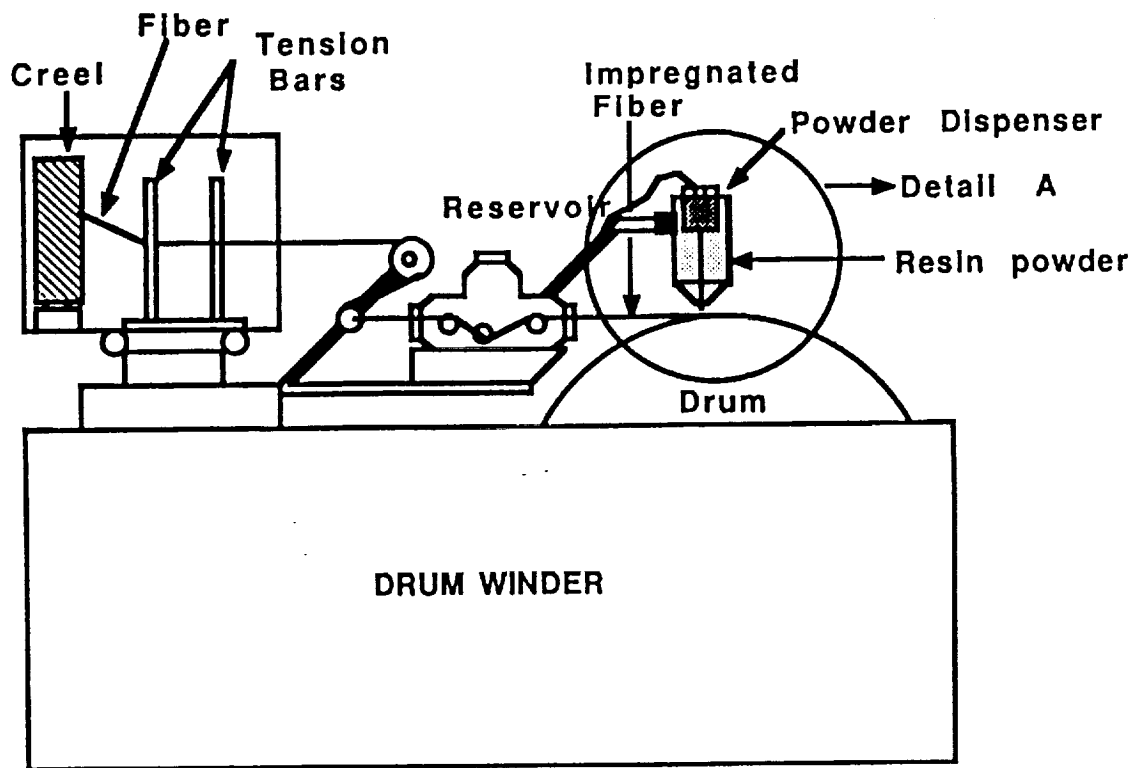


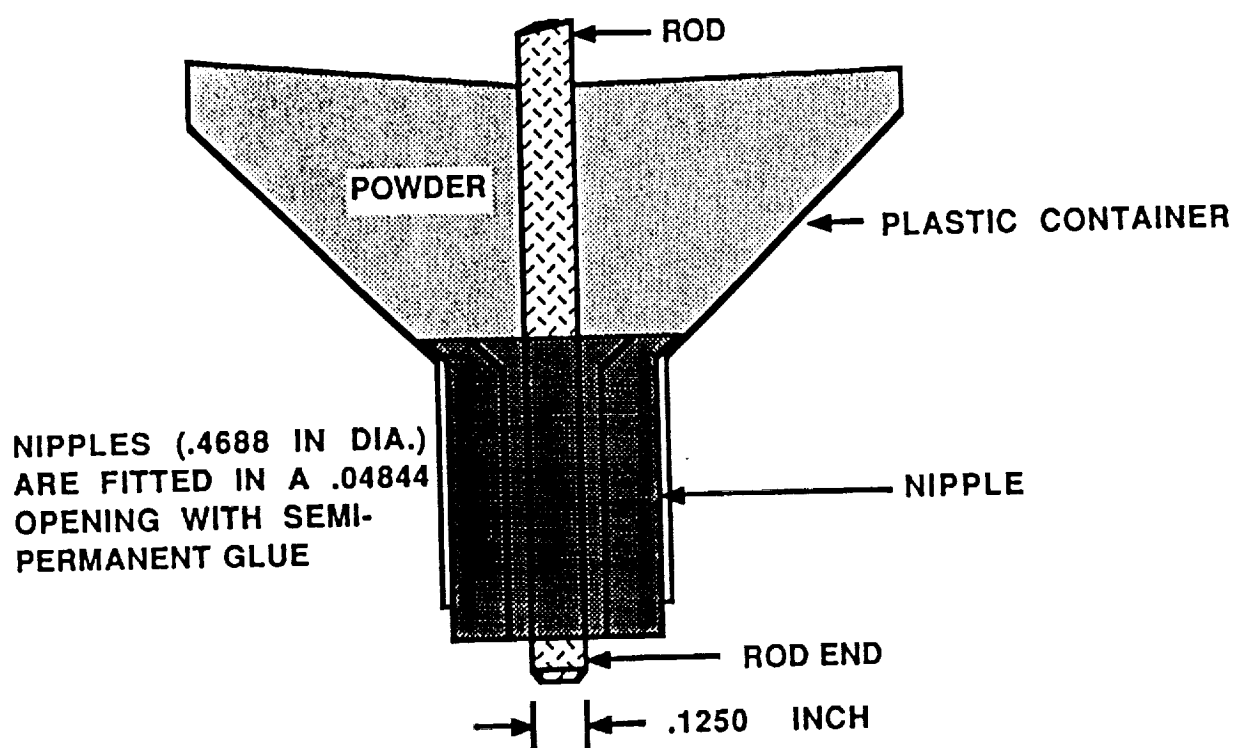
FIGURE 2



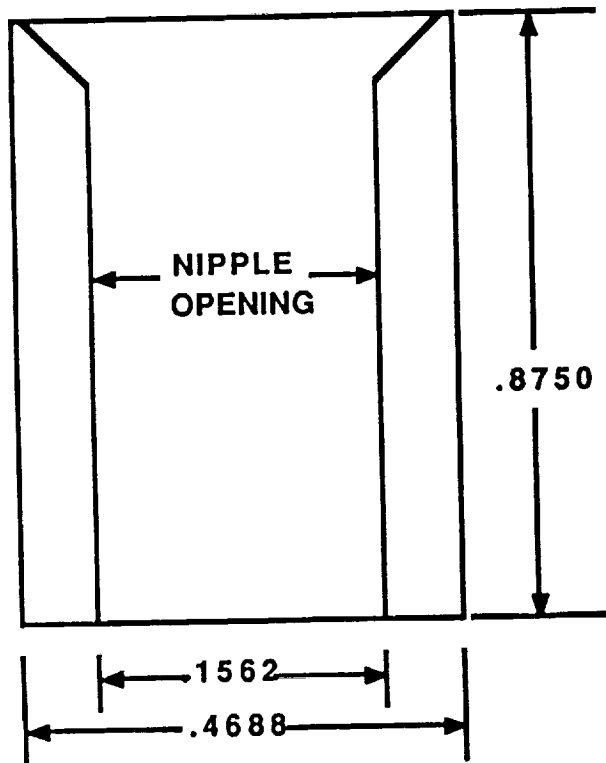
### POWDER DISPENSER ASSEMBLY

FIGURE 3

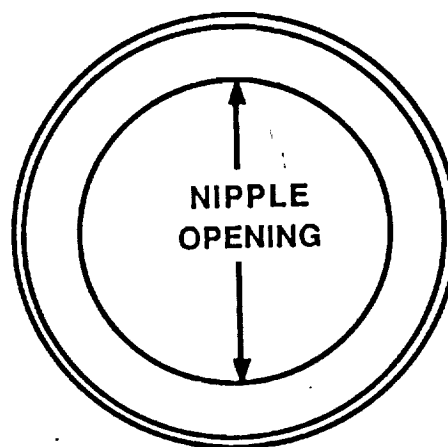




**NIPPLE FRONT/SIDE VIEW**



**NIPPLE TOP VIEW**

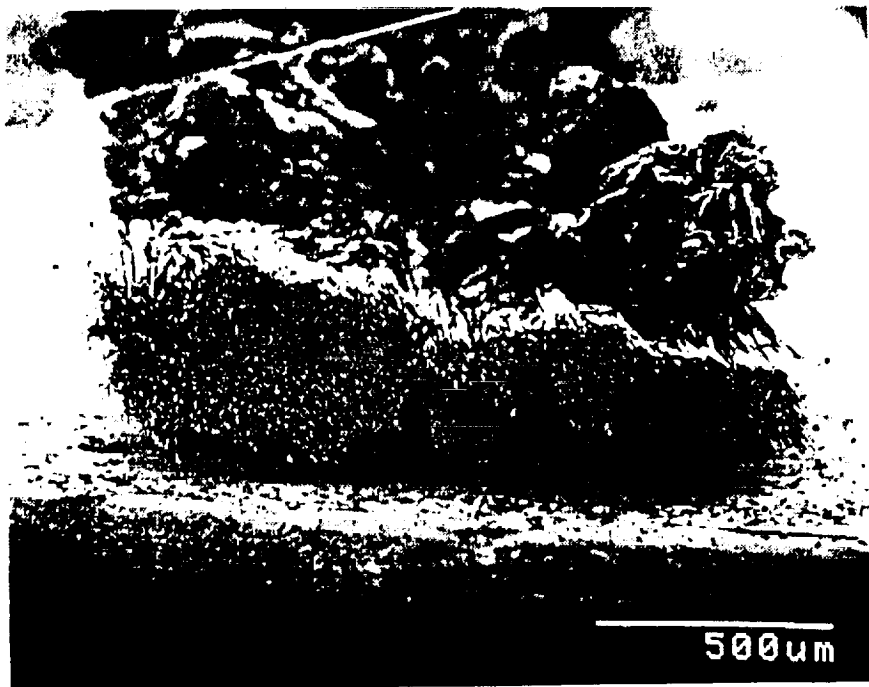


**NIPPLE OPENING SIZES IN USE ARE**

1. .1562
2. .1719
3. .1875
4. .2031

## **POWDER DISPENSER DETAILS**

**FIGURE 4**



SEM PHOTOMICROGRAPH OF RP46-5218/IM-7 PREPREG

FIGURE 5

ORIGINAL PAGE IS  
OF POOR QUALITY

# STRENGTH

Rate = 0.05 in./min (1.27 mm/min)

IM-7 Fiber

$V_f = 0.6$

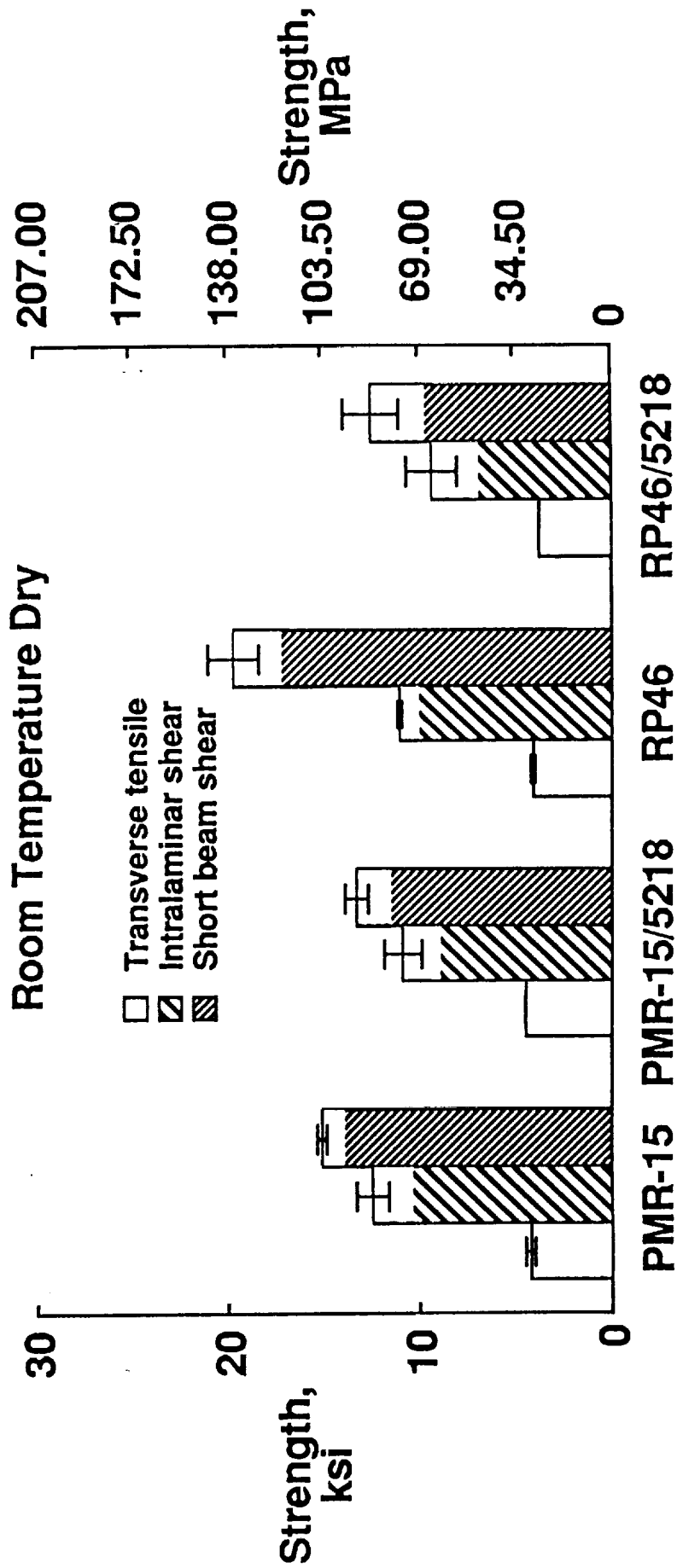


FIGURE 6

# STRENGTH

Rate = 0.05 in./min (1.27 mm/min)

IM-7 Fiber

$V_f = 0.6$

Room Temperature Dry

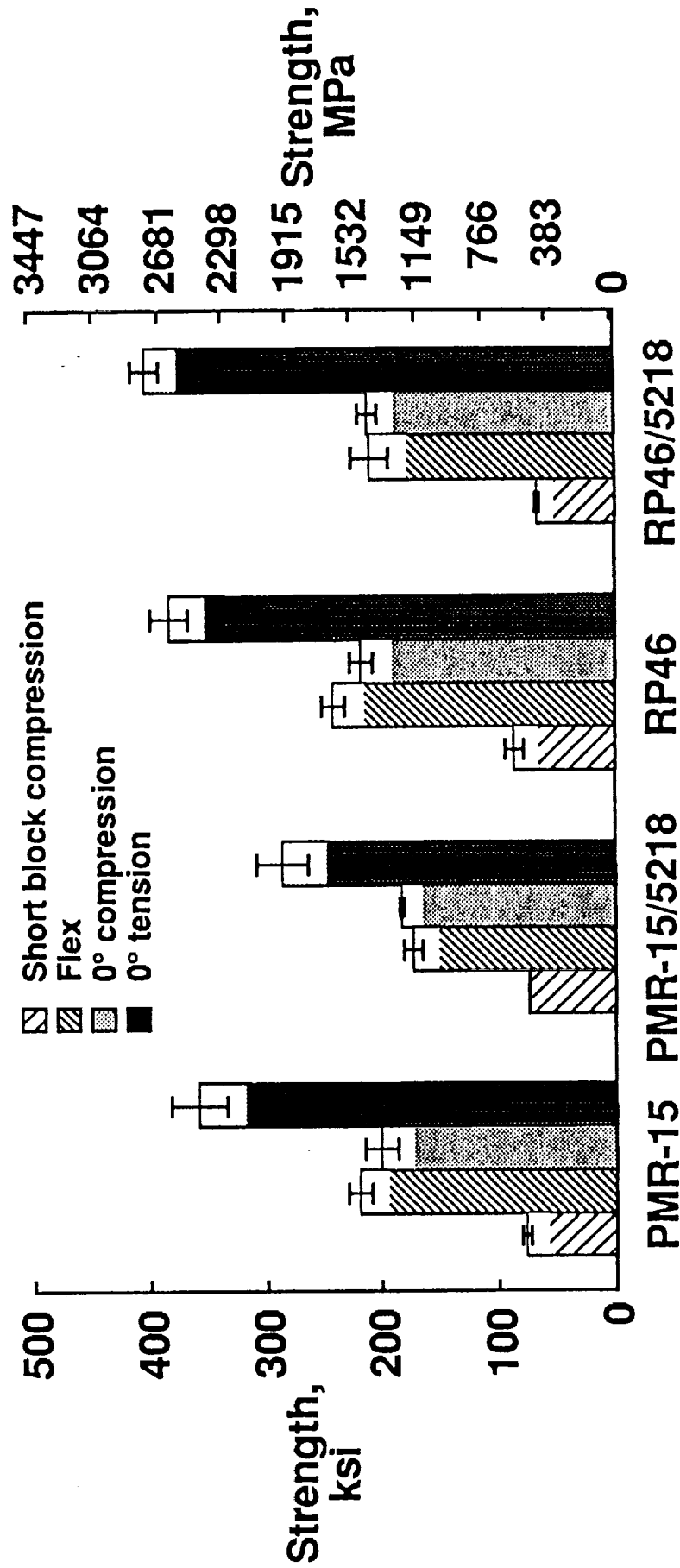


FIGURE 7

# MODULUS

Rate = 0.05 in./min (1.27 mm/min)

IM-7 Fiber

$V_f = 0.6$

Room Temperature Dry

- ▨ Intralaminar shear
- Transverse tensile
- ▧ Short block compression
- ▩ Flex
- 0° tension
- ▤ 0° compression

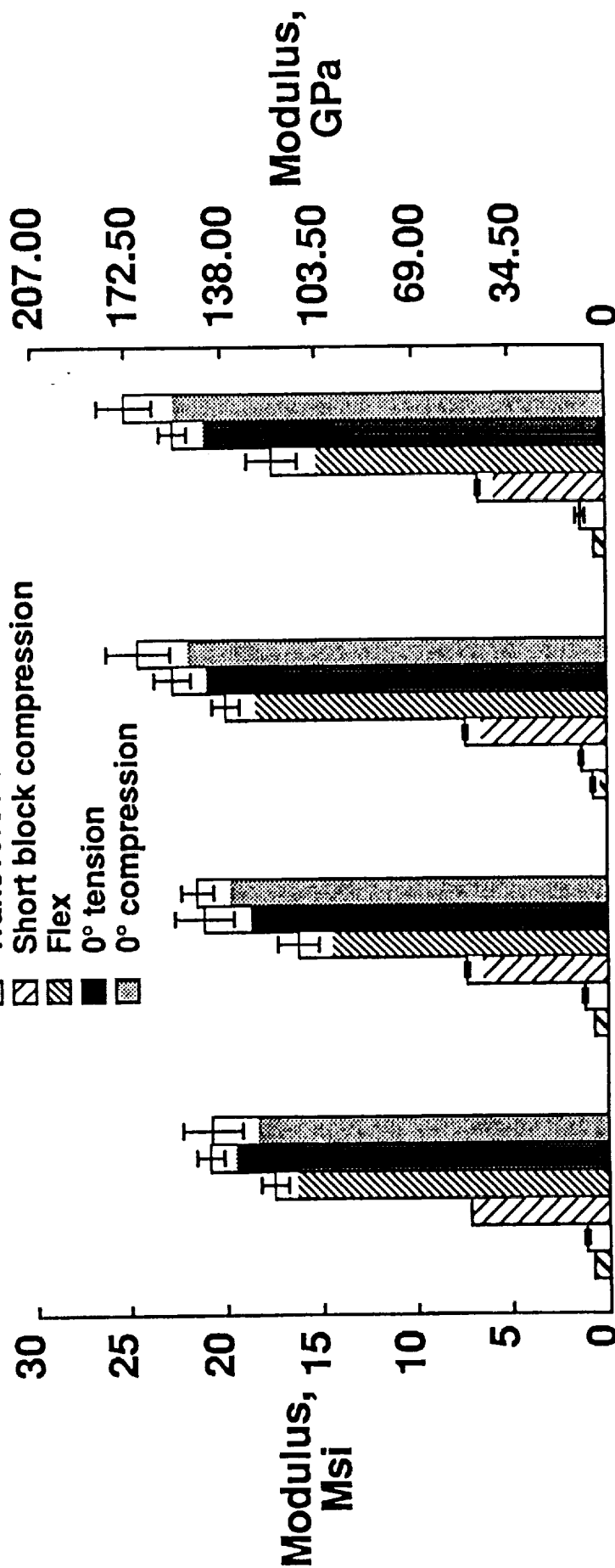


FIGURE 8

# FAILURE STRAIN/DEFLECTION

Rate = 0.05 in./min (1.27 mm/min)

IM-7 Fiber

$V_f = 0.6$

Room Temperature Dry

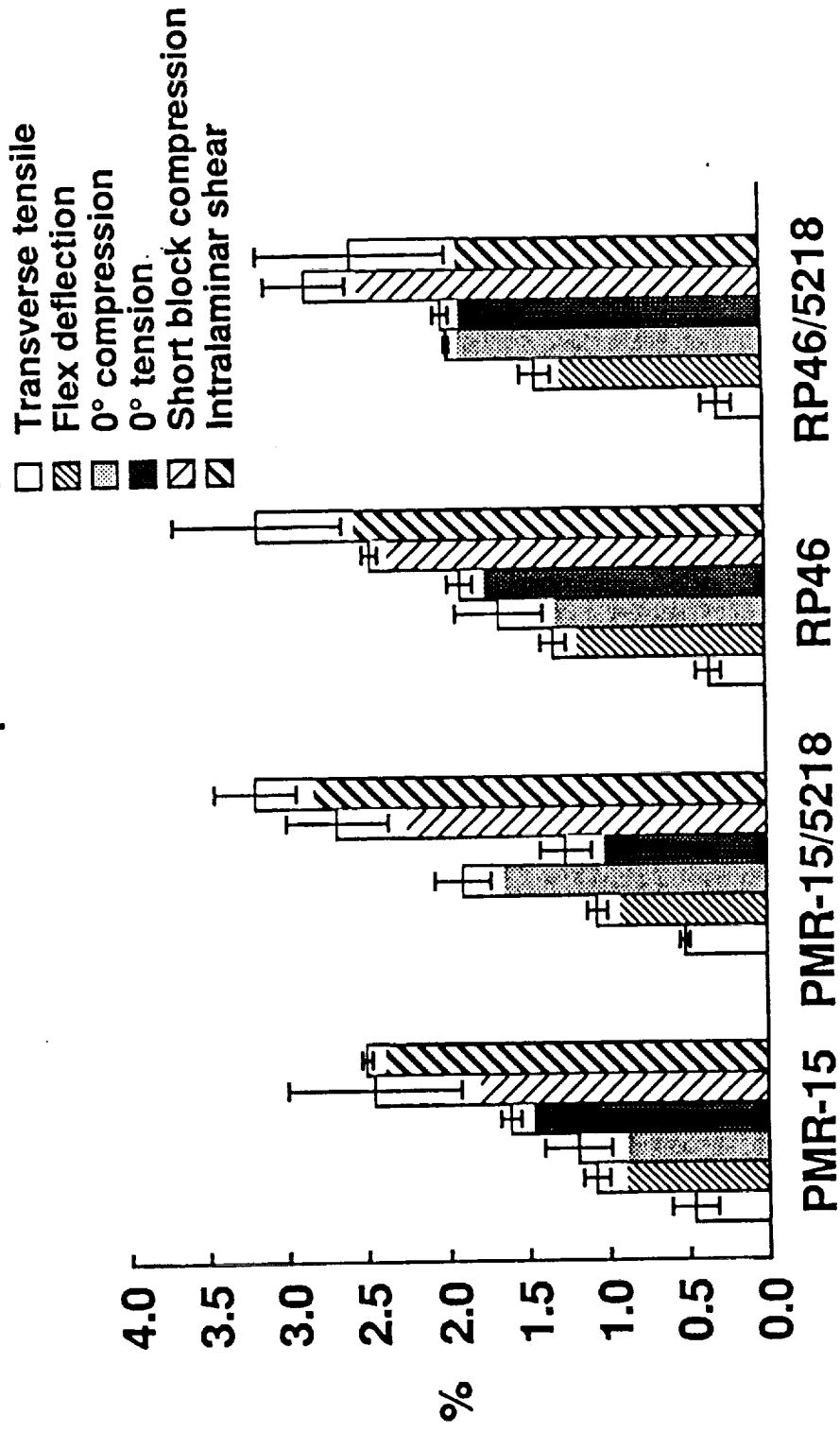


FIGURE 9

# INTERLAMINAR FRACTURE TOUGHNESS

Rate = 0.05 in./min (1.27 mm/min)

IM-7 Fiber

$V_f = 0.6$

Room Temperature Dry

(0)<sub>24</sub> with 0.0005 in. (0.0127 mm)

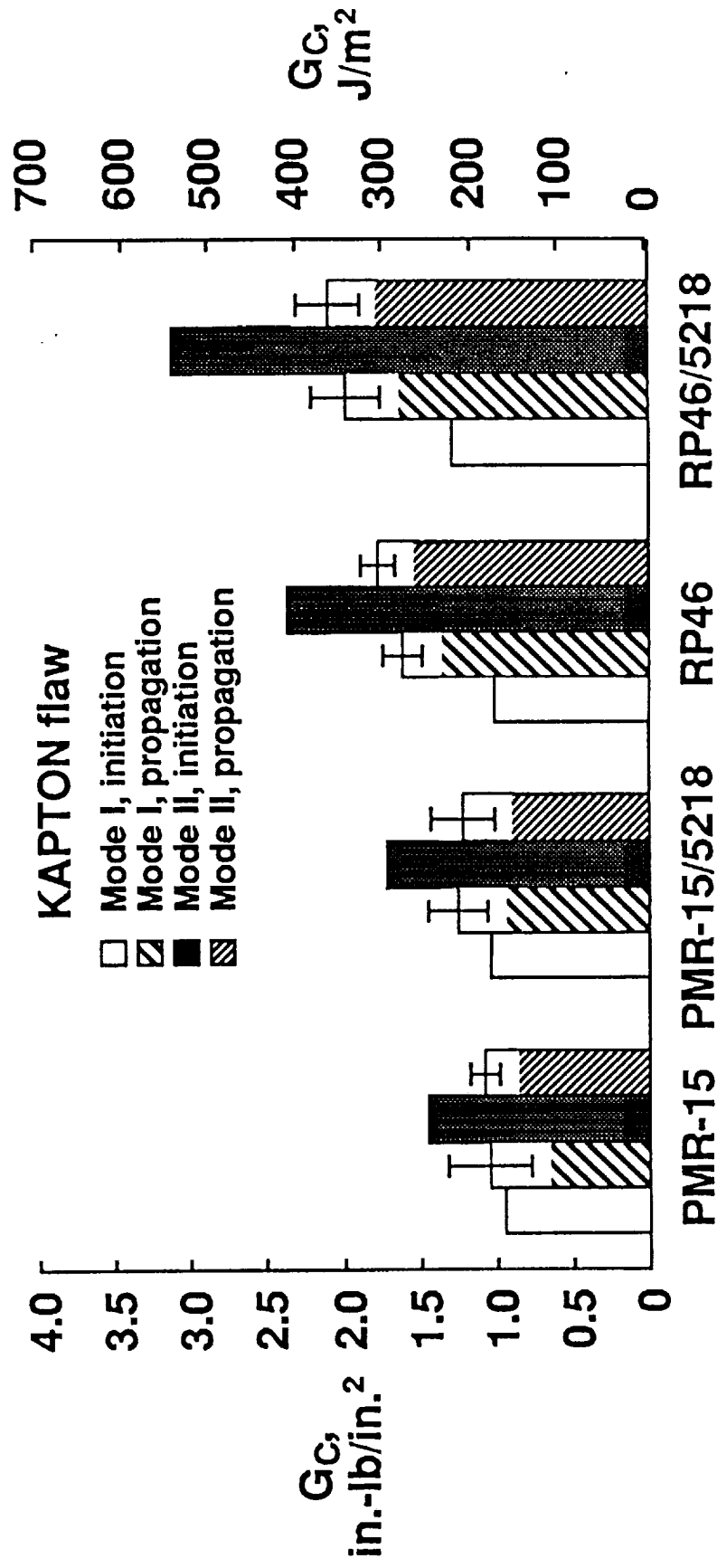


FIGURE 10

## RP46 PROCESS STANDARDIZATION DETAILS

SOLIDS CONTENT (*1), %	SOLUTION VISCOSITY (*1 *2), CPS	SOLUTION DENSITY (*1), G/CC	B-STAGED PER PLY THICKNESS (*3), IN	CURED LAMINATE Vf (*4), %	POSTCURED LAMINATE Vf (*5), %	POSTCURED PER PLY THICKNESS (*5), IN
34.0	4.1	0.880	0.014	60.1	62.5	0.0061
38.7	4.5	0.893	0.017	58.3	60.2	0.0067
41.6	6.7	0.937	0.020	57.0	58.1	0.0071

- \*1 in Methanol
- \*2 Brookfield viscosity at 25 ° C
- \*3 1 hour at 200 ° C
- \*4 Standard Processing Cycle
- \*5 Modified Processing Cycle

TABLE 1



# TEST MATRIX

Test Conditions: RTD,  $v_f = 0.6$  Rate = 0.05 in./min

#	Laminate	Loading	Size			Quantity
			Length, in.	Width, in.	Thickness, in.	
1.	(0) <sub>n</sub>	0° flexure	3.0	0.5	0.08	10
2.	(0) <sub>n</sub>	Short beam shear	0.75	0.25	0.125	10
3.	(0) <sub>8</sub>	Longitudinal tension	6.0	0.5	0.048	5
4.	(0) <sub>16</sub>	Longitudinal compression (IITRI)	6.0	1.0	0.10	5
5.	(90) <sub>16</sub>	Transverse tension	6.0	1.0	0.10	5
6.	(±45) <sub>2s</sub>	Intralaminar shear (tensile)	6.0	0.75	0.05	5
7.	(-45/0/45/90) <sub>4s</sub>	Short block compression	1.75	1.5	0.20	3
8.	(0) <sub>24</sub> with 0.0005 in. KAPTON insert at midplane	DCB	6.0	1.0	0.16	2
9.	(0) <sub>24</sub> with 0.0005 in. KAPTON insert at midplane	ENF	6.0	1.0	0.16	2
10.	(-45/0/45/90) <sub>4s</sub>	CAI (Boeing)	6.0	4.0	0.20	2

TABLE 2